



Published in final edited form as:

Dev Biol. 2020 November 01; 467(1-2): 30–38. doi:10.1016/j.ydbio.2020.07.013.

Cell culture system to assay candidate genes and molecular pathways implicated in congenital diaphragmatic hernias

Eric L. Bogenschutz^{1,2}, Elizabeth M. Sefton^{1,2}, Gabrielle Kardon^{1,*}

¹Department of Human Genetics, University of Utah, Salt Lake City, UT 84112

²Co-first authors

Abstract

The mammalian muscularized diaphragm is essential for respiration and defects in the developing diaphragm cause a common and frequently lethal birth defect, congenital diaphragmatic hernia (CDH). Human genetic studies have implicated more than 150 genes and multiple molecular pathways in CDH, but few of these have been validated because of the expense and time to generate mouse mutants. The pleuroperitoneal folds (PPFs) are transient embryonic structures in diaphragm development and defects in PPFs lead to CDH. We have developed a system to culture PPF fibroblasts from E12.5 mouse embryos and show that these fibroblasts, in contrast to the commonly used NIH 3T3 fibroblasts, maintain expression of key genes in normal diaphragm development. Using pharmacological and genetic manipulations that result in CDH *in vivo*, we also demonstrate that differences in proliferation provide a rapid means of distinguishing healthy and impaired PPF fibroblasts. Thus, the PPF fibroblast cell culture system is an efficient tool for assaying the functional significance of CDH candidate genes and molecular pathways and will be an important resource for elucidating the complex etiology of CDH.

Keywords

CDH; fibroblasts; diaphragm; congenital diaphragmatic hernia; cell culture

INTRODUCTION

The diaphragm is a mammalian-specific skeletal muscle that is essential for the inspiration phase of respiration and separates the thoracic from the abdominal cavity. Defects in diaphragm development are relatively common, occurring in 1 in 3000 births (Stege et al., 2003). In congenital diaphragmatic hernias (CDHs), abdominal contents herniate through

*Corresponding author: gkardon@genetics.utah.edu.

AUTHOR CONTRIBUTIONS

E.M.S. and E.L.B. performed experiments, data analysis, and drafted the manuscript. E.L. B., E.M.S. and G.K. designed the research. G.K. revised and edited the manuscript.

Publisher's Disclaimer: This is a PDF file of an unedited manuscript that has been accepted for publication. As a service to our customers we are providing this early version of the manuscript. The manuscript will undergo copyediting, typesetting, and review of the resulting proof before it is published in its final form. Please note that during the production process errors may be discovered which could affect the content, and all legal disclaimers that apply to the journal pertain.

The authors declare no conflicts of interest.

weakened portions of the diaphragm into the thoracic cavity. As a result, lung development is impeded, leading to lung hypoplasia and high neonatal mortality (Pober, 2007). Genetic studies in humans have identified multiple chromosomal abnormalities and *de novo* mutations in numerous genes that may contribute to the etiology of CDH and have implicated the involvement of multiple molecular pathways (reviewed by Kardon et al., 2017). However validation that mutations in any of these candidate genes are functionally important or demonstration that a particular molecular pathway is critical for development of CDH has been a significant challenge.

The diaphragm develops primarily from two embryonic tissues (Merrell et al., 2015). The pleuroperitoneal folds (PPFs) are transient bilateral pyramidal structures derived from lateral plate mesoderm and located between the thoracic (pleural) and abdominal (peritoneal) cavities (Merrell et al., 2015) and ultimately give rise to the diaphragm's muscle connective tissue and central tendon. The somites are the source of migratory muscle progenitors which target the PPFs and subsequently give rise to the diaphragm's muscle (Allan and Greer, 1997; Babiuk et al., 2003; Dietrich et al., 1999; Sefton et al 2018). As the muscle progenitors enter the PPFs, the PPFs spread dorsally and ventrally to form a continuous sheet in which the central tendon differentiates in the central region and the muscle differentiates peripherally to form the radial array of costal myofibers (Merrell et al., 2015; Sefton et al., 2018). Importantly, the development of the PPFs has been found to regulate the overall morphogenesis of the diaphragm (Babiuk et al., 2003; Merrell et al., 2015; Sefton et al., 2018).

Recent studies have established that the PPFs not only control normal diaphragm development, but defects in PPF development lead to CDH. Several mouse conditional mutagenesis studies have demonstrated that CDH-implicated genes cause hernias when mutated in PPFs or their associated mesothelium (Carmona et al., 2016; Merrell et al., 2015; Paris et al., 2015). In addition, research from our lab on the transcription factor *Gata4*, a gene strongly implicated in CDH by human genetic studies (Arrington et al., 2012; Kammoun et al., 2018; Longoni et al., 2014; Longoni et al., 2012; Wat et al., 2012; Yu et al., 2012), has specifically demonstrated that deletion of *Gata4* in the PPF fibroblasts, and not muscle progenitors, leads to CDH with complete penetrance (Merrell et al., 2015). While deletion of CDH-implicated genes leads to herniation beginning at E16.5 in mouse (E60 in humans), these genes are required much earlier in the PPFs – between E10.5 and 12.5 (E28 - E40 in humans; Carmona et al., 2016; Merrell et al., 2015; Paris et al., 2015) and lead to cell-autonomous changes within the PPF fibroblasts and cell non-autonomous effects on muscle progenitors. With deletion of CDH genes, PPF fibroblasts exhibit decreased proliferation, increased apoptosis, and altered gene expression (Carmona et al., 2016; Merrell et al., 2015; Paris et al., 2015).

Defective PPFs, in turn, affect the proliferation of neighboring muscle progenitors to ultimately lead to weakened regions of the diaphragm that allow herniation (Merrell et al., 2015). Altogether these *in vivo* studies have established that changes in the proliferation, survival, and gene expression of PPFs between E10.5 and E12.5 are critical determinants of whether CDH develops.

Besides mutations in individual genes, alterations in molecular signaling pathways regulating diaphragm development have been implicated in CDH (Kardon et al., 2017). Multiple pathways, including FGF, Hedgehog, and Wnt/ β -catenin signaling have been implicated. Most notably, alterations in maternal vitamin A or its derivative retinoic acid (RA) in the embryo have been proposed to be a potent source of CDH (Clugston et al., 2010a). RA is synthesized from vitamin A (retinol) via a two-step oxidation process: alcohol or retinol dehydrogenases convert retinol to all-trans-retinal and retinaldehyde dehydrogenases (primarily ALDH1A2 – formerly known as RALDH2 – in the embryo) converts all-trans-retinal to all-trans-retinoic acid (RA or ATRA) (Shannon et al., 2017). RA functions as either a paracrine or autocrine signal, binding retinoic acid receptors to form heterodimer complexes with retinoid receptors and activate transcription (Cunningham and Duester, 2015; Rhinn and Dollé, 2012; Shannon et al., 2017). The importance of RA signaling in CDH was first demonstrated in rodents where low maternal vitamin A (Anderson, 1941; Wilson et al., 1953) or environmental teratogens that interfere with RA signaling induces diaphragmatic hernias in offspring (Babiuk et al., 2004; Clugston et al., 2010a; Clugston et al., 2010b; Mey et al., 2003; Noble et al., 2007). In addition, babies born with CDH have been found to have low retinol and retinol binding protein in their blood (Beurskens et al., 2010; Major et al., 1998). Finally, mutations in retinoic acid receptors in mice and humans have been associated with CDH (Golzio et al., 2007; Mendelsohn et al., 1994; Pasutto et al., 2007; You et al., 2005). Thus, both environmental perturbations of and genetic mutations in RA signaling have been implicated in CDH. Mechanistic insights into how disruptions in RA signaling cause CDH have largely come from delivery of teratogens to pregnant rodents. Nitrofen is a diphenyl ether herbicide that inhibits ALDH1A2 activity (Mey et al., 2003), and its delivery induces diaphragmatic hernias in embryos (Babiuk et al., 2004; Clugston et al., 2010a; Clugston et al., 2010b; Costlow and Manson, 1981; Mey et al., 2003; Noble et al., 2007; See et al., 2008). ALDH1A2 is strongly expressed in the PPFs (Clugston et al., 2010a; Mey et al., 2003), and nitrofen inhibits proliferation of PPF fibroblasts and overall PPF morphogenesis (Clugston et al., 2010b). These teratogen studies demonstrate that, like mutations in individual CDH-implicated genes, inhibition of RA signaling induces CDH via its inhibition of PPF growth and morphogenesis.

Overall, the etiology of CDH is heterogeneous, potentially involving more than 150 genes and multiple molecular pathways, but few of these genes and pathways have been functionally validated in mice as causative of diaphragmatic hernias (Kardon et al., 2017). This is in part due to the cost and time required to generate and analyze suitable mouse models. As the diaphragm is a mammalian-specific structure (Perry et al., 2010), rodents are the only widely used animal model to study CDH *in vivo*. Rodent *in vivo* studies indicate that the PPFs are critical for diaphragm development, and inhibition of early PPF growth and morphogenesis, via genetic mutations or inhibition of molecular signaling pathways, leads to CDH. Here, we develop a system to culture these early PPFs and show they maintain expression of key genes in normal diaphragm development. Furthermore, we validate that genetic and pharmacological manipulations known to cause hernias *in vivo* in mice lead to impaired growth of PPF fibroblasts *in vitro*. This cell culture system, in combination with pharmacological interventions and future gene knock-down and editing experiments, will allow for rapid screening of CDH candidate genes and molecular pathways. This culture

system will provide an important tool for prioritizing genes to functionally test *in vivo* in mice and ultimately target therapeutically.

MATERIALS AND METHODS

Cell culture, media, and reagents

NIH/3T3 cells were obtained from ATCC (CRL-1658). Embryos were dissected from pregnant CD-1 female mice mated with CD-1 males or pregnant *Gata4^{fl/fl}; Rosa^{mTmG/mTmG}* females mated with *Prx1Cre^{Tg/+}; Gata4^{del/+}* males. Staged E11.5 or E12.5 embryos were dissected from yolk sacs in sterile PBS and transferred to Ham's F-12 Nutrient Mixture (F-12) (Gibco). Embryos were trimmed with two cuts to isolate the trunk region: one cut across the embryo just caudal to the forelimbs and another cut across the embryo just cranial to the hindlimbs (and leaving liver attached to trunk). Developing heart and lungs were pulled out cranially from the thoracic cavity using forceps and the trunk trimmed to the base of the rib cage to expose the PPFs lying lateral to the vertebral column and on top of the liver. Trimmed trunks were pinned onto a Sylgard coated 6mm dish in media. Pairs of PPFs were isolated manually with forceps from the lateral body wall and from the underlying septum transversum and liver (Video 1) and then each pair placed in a single well in a 96-well plate (Eppendorf) containing 100 μ L of media. To promote growth of PPF fibroblasts, we used PPF growth media: Ham's F-12 Nutrient Mixture, 10% Fetal Bovine Serum (FBS), 50 μ g/mL Gentamycin (all from Gibco). To promote growth of PPF fibroblasts and myogenic cells, we used myogenic media: Ham's F-10 with L-glutamine (Caisson) or DMEM/F-12 GlutaMAX (Invitrogen), 10% FBS, 50 μ g/mL gentamycin, and 0.5 nM FGF. PPFs were grown in a 37°C incubator for 5 d, changing media in the wells every 2 d. After 5 d, cells were passaged by removing the media in the well, washing the cells with 100 μ l of F-12 media twice, then de-adhering cells by placing 100 μ l 0.25% trypsin-EDTA (Gibco) in each well with PPFs and incubating for 9 minutes at 37°C. Trypsin and cells were transferred from each well to a 1.5mL Eppendorf tubes and trypsin neutralized by adding 100 μ l of growth or myogenic media. Suspended cells were pelleted by centrifuging for 5 minutes at 340xg, trypsin and media removed, disaggregated cells were resuspended in 100 μ l growth or myogenic media and simply transferred to a new well on a 96-well plate. Cells were grown for another 5 d (with media changes every 5 d) and at a total of 10d in culture were passaged again. On this second passage, resuspended cells were counted and ~10,000 cells/well were seeded and grown for another 3 d. For nitrofen treatments, nitrofen (Sigma) and RA (Sigma) treatments, 28 pairs of PPFs were de-adhered after 5 days in culture using the same trypsin method, but pooled, counted, and seeded at ~10,000 cells/well of a 96-well plate. Cells were subjected to 4 treatment conditions: not-treated, DMSO, 1 nM RA, 100 μ M nitrofen, or 1nM RA plus 100 μ M nitrofen. RA was dissolved in DMSO to a stock concentration of 10 mM and then diluted to 1 nM in PPF growth media. Nitrofen was dissolved in DMSO to a stock concentration of 100 mM and then diluted to a 100 μ M in PPF growth media. For the combined RA and nitrofen treatment, nitrofen was diluted to 200 μ M and RA diluted to 2nM in PPF growth media and combined in equal volumes and applied to wells. In DMSO treatment, DMSO was added to PPF growth media at same concentration as in combined RA and nitrofen treatments. Fresh DMSO, RA, and nitrofen were added every 24 hours and media replaced every 2 d.

Cell growth analysis

Proliferating cells were imaged using the IncuCyte ZOOM which took 4 representative phase-contrast images per well every 2 hours. IncuCyte software was then used to analyze average confluency per well per time point to calculate cell growth over time. To control for differences in seeding densities between wells, fold changes of cell growth were calculated by dividing each treatment by the mean initial confluency at time 0. For GFP experiments, both phase and GFP images were taken by the IncuCyte ZOOM, with the same number of images and time intervals used. Both total cell percentage (from phase-contrast images) and GFP-positive cell percentages (from GFP images) were used to analyze growth of GFP+ cells compared with growth of all cells (from phase-contrast images).

RNA extraction, cDNA synthesis, and quantitative polymerase chain reaction (qPCR)

Total RNA was extracted with the *Quick-RNA* Microprep kit (Zymo, Irvine, CA) according to manufacturer's protocol. cDNA was synthesized using Applied Biosystems High-Capacity RNA-to-cDNA kit (ThermoFisher) from purified RNA according to manufacturer's protocol. qRT-PCR was used to analyze expression of *Gata4*, *Zfpn2*, *Nr2f2*, *Tbx5*, *Gata6*, *PDGFRa*, and *Pax7* using pre-validated primer sets (TaqMan, ThermoFisher; Table S1). 10 μ l or 20 μ l reaction volumes were prepared using TaqMan Fast Advanced Master Mix (ThermoFisher). The amplification was performed under the following conditions: 20 seconds at 95°C followed by 40 cycles at 95°C for 1 second and 60°C for 20 seconds. Gene expression levels were normalized against *18S* ribosomal RNA for each sample and fold changes were calculated using 2^{-Ct} method (Schmittgen and Livak, 2008) by setting the expression levels of each gene at stage-matched harvest as 1. Data collected from 2-5 biological replicates was calculated and plotted as average fold changes with standard error of the mean (SEM).

Statistical Analysis

Data are presented as mean \pm SEM. One-way analysis of variance (ANOVA) was used to determine differences in gene expression. If significant, a Holm-Sidak post hoc test was used. For growth comparisons between either chemical treatments or genotype, repeated ANOVA analysis was run on the log₂ fold change of either cell confluence (Fig. 4D) or the log₂ fold change of GFP cells over total cells (Fig. 4B) to normalize the distribution of cell growth over time.

RESULTS

Early pleuroperitoneal folds can be isolated and expanded in culture

PPF fibroblasts are critical in both diaphragm development and an defects in PPF development lead to CDH. Because defects in proliferation and the morphogenetic spread of early PPF fibroblasts are lead to CDH *in vivo* (Carmona et al., 2016; Clugston et al., 2010b; Merrell and Kardon, 2013; Paris et al., 2015), we endeavored to set up an *in vitro* system to determine whether E11.5-E12.5 PPF fibroblasts can be cultured and maintain their ability to proliferate and spread. PPFs at this stage are bilateral pyramidal structures composed predominantly of fibroblasts and a smaller number of muscle progenitors which have

migrated into the PPFs (Sefton et al., 2018). The PPFs are visibly distinct by E11.5, and E11.5 - E12.5 PPFs are able to be manually dissected from the underlying liver with forceps under a dissecting microscope (Fig. 1A, Video 1). Isolated pairs of PPFs are removed with sterile forceps and then plated whole, ventral-side down, on tissue-culture treated 96 well plates with PPF growth media (F12 media, 10% FBS and 50 µg/ml Gentamicin). Once plated, the PPFs proliferate and spread across the well, similar to PPFs *in vivo* (Fig. 1B; Video 2). While E11.5 – E12.5 PPFs initially contain muscle progenitors, we found that these growth conditions do not favor myogenic cells. Muscle progenitors, which express Pax7, are neither present (Fig. S1) nor differentiate into myotubes after 5 days of culture. Thus these conditions allow us to specifically assess the proliferation and spread of PPF fibroblasts.

Our culture conditions allow E12.5 PPF fibroblasts to successfully grow for at least 14 d in culture. During the initial culture of the intact PPFs, cells expand radially, but after 5 d in culture PPF cells become highly confluent and stop growing; at this point PPF fibroblasts are dissociated from each well, disaggregated, resuspended, and re-plated at an even density in a new well. The PPF fibroblasts can then be grown an additional 5 d, passaged, splitting cells from 1 well into 2-3 wells (with ~10,000 cells seeded at an even density in each well) and grown for a final 3-4 d. After the first passage at 5d or after the second passage at a total of 10 d in culture, we imaged and monitored cell proliferation for 96 hours using a Sartorius IncuCyte ZOOM live cell imager (Fig. 1C-F, Fig. S2). In addition, we compared the growth of PPF fibroblasts with NIH 3T3 fibroblast cells, immortalized fibroblasts derived from Swiss mouse embryonic fibroblasts (Todaro and Green, 1963), that were grown and imaged on the same 96 well plate (Fig. 1D, Fig. S2B). As expected, the NIH 3T3 fibroblasts grow under these conditions with little variability and double every 25 h (+/- 1.4 h, Fig. 1D, Fig. S2B). The PPFs initially grow more variably in culture (Fig 1E, Fig. S2C). After 5 d in culture PPFs double every 21 h (+/- 2.2 h) and after 10 d in culture they continue to double at this same rate, although with less variability (21 h +/- 0.8 h, Fig. 1 C-D). We have been able to continuously expand PPF fibroblasts from the initial 5,000 cells/pair of E12.5 PPFs, through 4 passages, to 1,000,000 PPF fibroblasts. Thus, we demonstrate that PPFs can be successfully isolated and reliably grown in culture with a consistent growth rate.

Maintaining muscle progenitors in combination with PPF fibroblasts may be important for assaying phenotypes associated with the interaction between myogenic cells and fibroblasts. PPFs grown in PPF growth media gradually lose any Pax7+ myogenic progenitors present in the initial PPF explant (Fig. S1). To optimize conditions for myogenic cells, we cultured PPFs from *Pax3^{Cre/+}; Rosa^{nTnG/+}* mice. *Pax3^{Cre}* recombines in the somites and earliest muscle progenitors (Engleka et al., 2005). *Pax3^{Cre}* in combination with the Cre-responsive reporter *Rosa^{nTnG}* (in which all cells express nuclear Tomato and in response to Cre cells express nuclear GFP) labels all myogenic cells with GFP and PPF fibroblasts with Tomato. E12.5 PPFs from *Pax3^{Cre/+}; Rosa^{nTnG/+}* mice were cultured with 0.5 nM FGF (Farina et al., 2012) and 10% fetal bovine serum in either F-10 or F-12/DMEM media (1:1) to compare muscle progenitor survival over time. Over 5 d in culture, while numbers of GFP+ myogenic cells decreased in F-10 (Fig. 2A-B), the numbers of GFP+ myogenic cells increased in F-12/DMEM (Fig. 2C-D). Thus, for analyses requiring co-culture of myogenic cells and PPF fibroblasts, F-12/DMEM media with 10% FBS and FGF is a suitable media.

E12.5 PPF fibroblasts maintain expression of key diaphragm genes for at least 10 days in culture

A robust PPF cell culture model of early diaphragm development and CDH requires that expression of key genes important for normal diaphragm development (and aberrant in CDH) is maintained in wild-type PPF fibroblasts during culture. As such, we examined the expression of multiple diaphragm genes during culture of E12.5 PPF fibroblasts. We included the transcription factors *Gata4* (Jay et al., 2007; Merrell et al., 2015; Yu et al., 2012), *Gata6* (Yu et al., 2014), and *Tbx5* (which can bind cooperatively with *Gata4* to transactivate genes; Ang et al., 2016; Valasek et al., 2011); *Gata4* co-factor *Zfpm2* (Ackerman et al., 2005; Chlon and Crispino, 2012); and the orphan nuclear receptor *Nr2f2* (which binds and interacts with *Gata4* and *Zfpm2*; Huggins et al., 2001; You et al., 2005). Together the proteins encoded by these genes likely form an essential transcriptional network regulating normal diaphragm development. In addition, each one of these genes when mutated causes CDH. We also included the receptor *Pdgfra* which labels muscle connective tissue fibroblasts and is implicated in CDH (Bleyl et al., 2007; Uezumi et al., 2010). We found that all of these genes are expressed in E12.5 PPFs at harvest and *Gata4*, *Zfpm2*, *Nr2f2*, *Tbx5*, and *Gata6* do not change significantly after 5 or 10 d in culture (Fig. 3A-E). Only *Pdgfra* is somewhat altered during culture, as it is transiently downregulated after 5 d in culture but recovers expression following 10 d in culture (Fig. 3F). In contrast, while NIH 3T3 fibroblasts express similar levels of *Gata4*, *Gata6*, *Nr2f2*, and *Pdgfra* as E12.5 PPFs at harvest, they expressed significantly lower levels of *Zfpm2* and undetectable levels *Tbx5* (Fig. 3A-F). As regulation of *Gata4* transcriptional activity by *Zfpm2* and *Tbx5* is essential for regulating normal diaphragm development, this suggests that the transcriptional activity of NIH 3T3 cells will differ significantly from that of PPF fibroblasts. Thus, these experiments show that E12.5 PPF fibroblasts, and not NIH 3T3 fibroblasts, largely maintain expression of a network of key diaphragm genes after 10 d in culture.

As early developmental events are critical to the development of CDH (Carmona et al., 2016; Merrell et al., 2015; Paris et al., 2015), we also analyzed gene expression in cultured E11.5 PPFs (Fig. S3). First, we compared E11.5 to E12.5 PPFs at harvest and found no significant differences in expression of the important diaphragm genes (Fig. S2G). However after 5 or 10 d in culture, while expression of *Gata4* and *Gata6* are maintained (Fig. S3A-B), *Zfpm2*, *Tbx5*, *Nr2f2*, and *PDGFRa* are significantly reduced in E11.5 PPF fibroblasts (Fig. S3C-F). The reduced expression of multiple critical genes during culture of E11.5 PPFs indicates that these younger PPFs are not adequate as a cell culture model. Instead E12.5 PPF fibroblasts, but not E11.5 PPF or NIH 3T3 fibroblasts, continue to express important diaphragm genes in culture and likely serve as a good *in vitro* system for studying development of the diaphragm and CDH.

Genetic and pharmacological manipulations that lead to CDH in vivo cause decreased PPF proliferation in vitro.

Rodent *in vivo* studies demonstrate that inhibition of early PPF growth and spread, via genetic mutations or pharmacological inhibition of molecular signaling pathways, leads to CDH (Clugston et al., 2010b; Merrell et al., 2015; Paris et al., 2015). These studies suggest that reduction in the proliferation of early PPF cells may be a common feature of CDH

etiology. Therefore, we sought to determine whether a genetic mutation and pharmacological inhibition of a signaling pathway known to cause CDH *in vivo* would be recapitulated as changes in E12.5 PPF proliferation *in vitro*.

Mutations in *Gata4* have been strongly implicated by human genetic studies to cause CDH (e.g. Yu et al., 2013), and our lab has demonstrated in mice *in vivo* that loss of *Gata4* in PPF cells leads to decreased proliferation of PPF cells at E12.5 and CDH after E16.5 (Merrell et al., 2015). To test whether genetic loss of *Gata4* leads to decreased proliferation of PPFs *in vitro*, we harvested E12.5 PPFs from embryos in which either one (*Prx1Cre^{Tg/+};Gata4^{fl/+};Rosa^{mTmG/+}*) or both alleles (*Prx1Cre^{Tg/+};Gata4^{del/fl};Rosa^{mTmG/+}*) of *Gata4* were deleted with the *Prx1Cre* transgene that is expressed in PPFs (Logan et al., 2002). As previously noted (Merrell et al., 2015), the *Prx1Cre* transgene does not recombine in all PPF cells by E12.5. Thus the Cre-responsive *Rosa^{mTmG}* reporter (Muzumdar et al., 2007) was used to identify GFP+ PPF fibroblasts in which the Cre protein was expressed and either one or two *Gata4* alleles was deleted. In order to determine the effects of *Gata4* deletion on proliferation of PPF fibroblasts, we analyzed growth of all PPFs (with phase images) and growth of GFP+ PPFs (with GFP fluorescence images) using the IncuCyte ZOOM live cell imager (representative images in Fig. 4A). We compared the fold change in the GFP+ PPF fibroblasts (% confluence at time T/% confluence at time 0) in which one or two alleles of *Gata4* was deleted with the fold change in all PPF fibroblasts and plotted this ratio over time. We found that the proportion of GFP+ PPF fold change relative to the total cell fold change decreased with time when both alleles of GFP were deleted (red line versus blue line in Fig. 4B). By repeated measures ANOVA, this difference is statistically significant when comparing proliferation during 48-90 hours (Fig. 4B). These data indicate that loss of the important CDH gene *Gata4* inhibits proliferation of E12.5 PPF fibroblasts in culture, recapitulating the effects seen *in vivo*. These data suggest that mutations in other genes causing CDH *in vivo* will lead to detectable changes in PPF fibroblasts proliferation.

RA signaling is an important regulator of normal diaphragm development and when inhibited causes CDH (Clugston et al., 2010a). Pharmacological inhibition of RA synthesis via administration to pregnant females of nitrofen, a herbicide that inhibits ALDH1A2 (Alles et al., 1995; Kling et al., 2010; Mey et al., 2003), inhibits growth of the PPFs to ultimately cause CDH in embryos (Costlow and Manson, 1981; Nakao and Ueki, 1987). To test whether nitrofen similarly affects PPF proliferation *in vitro*, we cultured E12.5 PPFs in the presence of 100 μ M nitrofen. Compared with untreated or vehicle-treated PPFs, nitrofen treatment significantly decreased PPF proliferation (Fig. 4C-D). Furthermore, this impairment of PPF proliferation was rescued by addition of 1 nM RA. Thus the effects of pharmacological inhibition of RA *in vivo* are similarly recapitulated as changes in PPF proliferation *in vitro*.

In summary, these two sets of experiments demonstrate that genetic manipulations and pharmacological inhibitors that cause CDH *in vivo* have a measurable effect on proliferation of E12.5 PPFs when cultured *in vitro* and suggests that this culture system will be an effective tool for functional testing candidate CDH genes and molecular pathways.

DISCUSSION

The etiology of CDH is complex and potentially involves mutations in many genes and aberrations in multiple signaling pathways. However, functional testing of candidate genes and molecular pathways for their role in CDH etiology has been limited by the substantial time and expense to generate *in vivo* mouse models. We have developed a more rapid and cost-effective *in vitro* system to carry out functional tests. We have optimized a protocol to isolate and culture E12.5 mouse PPF fibroblasts, allowing visualization and quantification of the cell population driving normal diaphragm morphogenesis and CDH. In culture, PPF fibroblasts proliferate and maintain expression of key diaphragm development genes. Furthermore, genetic mutations and pharmacological manipulations that lead to CDH *in vivo* impair PPF proliferation *in vitro*. This *in vitro* system, in combination with the large number of pharmacological tools currently available, will enable a wide variety of candidate signaling pathways to be quickly tested and give mechanistic insights into the regulation of PPF growth and development of CDH. In the future, as CRISPR-Cas9 genome editing is optimized for primary cells, mutations in candidate CDH genes can be engineered directly into wild-type PPFs to test their possible function.

Supplementary Material

Refer to Web version on PubMed Central for supplementary material.

ACKNOWLEDGEMENTS

We thank B Collins for critical reading of the manuscript and O Balcioglu and B Spike for use of their IncuCyte ZOOM cell imager.

FUNDING

This work was supported by the National Institutes of Health (R01HD087360), March of Dimes (6FY15203), Wheeler Foundation, and Utah Genome Project Functional Analysis Pilot grants to G. Kardon. E.L. Bogenschutz was supported by the University of Utah Genetics Training grant (T32 GM007464). E.M. Sefton is supported by National Institutes of Health (F32 HD093425).

REFERENCES

- Ackerman KG, Herron BJ, Vargas SO, Huang H, Tevosian SG, Kochilas L, Rao C, Pober BR, Babiuk RP, Epstein JA, Greer JJ, Beier DR, 2005 Fog2 Is required for normal diaphragm and lung development in mice and humans. *PLoS Genet.* 1, e10.
- Allan DW, Greer JJ, 1997 Embryogenesis of the phrenic nerve and diaphragm in the fetal rat. *J. Comp. Neurol* 382, 459–468. [PubMed: 9184993]
- Alles AJ, Losty PD, Donahoe PK, Manganaro TF, Schnitzer JJ, 1995 Embryonic cell death patterns associated with nitrofen-induced congenital diaphragmatic hernia. *J. Pediatr. Surg* 30, 353–360. [PubMed: 7537810]
- Anderson DH, 1941 Incidence of congenital diaphragmatic hernia in the young of rats bred on a diet deficient in vitamin A. *Am. J. Dis. Child* 62, 888–889.
- Ang YS, Rivas RN, Ribeiro AJ, Srivas R, Rivera J, Stone NR, Pratt K, Mohamed TM, Fu JD, Spencer CI, Tippens ND, Li M, Narasimha A, Radzinsky E, Moon-Grady AJ, Yu H, Pruitt BL, Snyder MP, Srivastava D, 2016 Disease Model of GATA4 Mutation Reveals Transcription Factor Cooperativity in Human Cardiogenesis. *Cell* 167, 1734–1749 e1722. [PubMed: 27984724]
- Arrington CB, Bleyl SB, Matsunami N, Bowles NE, Leppert TI, Demarest BL, Osborne K, Yoder BA, Byrne JL, Schiffman JD, Null DM, DiGeronimo R, Rollins M, Faix R, Comstock J, Camp NJ,

- Leppert MF, Yost HJ, Brunelli L, 2012 A family-based paradigm to identify candidate chromosomal regions for isolated congenital diaphragmatic hernia. *Am J Med Genet A* 158A, 3137–3147. [PubMed: 23165927]
- Babiuk RP, Thebaud B, Greer JJ, 2004 Reductions in the incidence of nitrofen-induced diaphragmatic hernia by vitamin A and retinoic acid. *Am. J. Physiol. Lung Cell. Mol. Physiol* 286, L970–L973. [PubMed: 14729516]
- Babiuk RP, Zhang W, Clugston R, Allan DW, Greer JJ, 2003 Embryological origins and development of the rat diaphragm. *J. Comp. Neurol* 455, 477–487. [PubMed: 12508321]
- Beurskens LWJE, Tibboel D, Lindemans J, Duvekot JJ, Cohen-Overbeek TE, Veenma DCM, de Klein A, Greer JJ, Steegers-Theunissen RPM, 2010 Retinol status of newborn infants is associated with congenital diaphragmatic hernia. *Pediatrics* 126, 712–720. [PubMed: 20837596]
- Bleyl SB, Moshrefi A, Shaw GM, Saijoh Y, Schoenwolf GC, Pennacchio LA, Slavotinek AM, 2007 Candidate genes for congenital diaphragmatic hernia from animal models: sequencing of FOG2 and PDGFR alpha reveals rare variants in diaphragmatic hernia patients. *Eur. J. Hum. Genet* 15, 950–958. [PubMed: 17568391]
- Carmona R, Cañete A, Cano E, Ariza L, Muñoz-Chápuli R, 2016 Conditional deletion of WT1 in the septum transversum mesenchyme causes congenital diaphragmatic hernia in mice. *eLife* 19, e16009.
- Chlon TM, Crispino JD, 2012 Combinatorial regulation of tissue specification by GATA and FOG factors. *Development* 139, 3905–3916. [PubMed: 23048181]
- Clugston RD, Zhang W, Álvarez S, de Lera AR, Greer JJ, 2010a Understanding abnormal retinoid signaling as a causative mechanism in congenital diaphragmatic hernia. *Am. J. Respir. Cell Mol. Biol* 42, 276–285. [PubMed: 19448158]
- Clugston RD, Zhang W, Greer JJ, 2010b Early development of the primordial mammalian diaphragm and cellular mechanisms of nitrofen-induced congenital diaphragmatic hernia. *Birth Defects Res. A Clin. Mol. Teratol* 88, 15–24. [PubMed: 19711422]
- Costlow R, Manson J, 1981 The heart and diaphragm: target organs in the neonatal death induced by nitrofen (2,4-dichlorophenyl-p-nitrophenyl ether). *Toxicology* 20, 209–227. [PubMed: 7256786]
- Cunningham TJ, Duester G, 2015 Mechanisms of retinoic acid signalling and its roles in organ and limb development. *Nat. Rev. Mol. Cell Biol* 16, 110–123. [PubMed: 25560970]
- Dietrich S, Abou-Rebyeh F, Brohmann H, Bladt F, Sonnenberg-Riethmacher E, Yamaai T, Lumsden A, Brand-Saberi B, Birchmeier C, 1999 The role of SF/HGF and c-Met in the development of skeletal muscle. *Development* 126, 1621–1629. [PubMed: 10079225]
- Engleka KA, Gitler AD, Zhang M, Zho DD, High FA, Epstein JA, 2005 Insertion of Cre into the Pax3 locus creates a new allele of Splotch and identifies unexpected Pax3 derivatives. *Dev. Biol* 280, 396–406. [PubMed: 15882581]
- Farina NH, Hausburg M, Betta ND, Pulliam C, Srivastava D, Cornelison D, Olwin BB, 2012 A role for RNA post-transcriptional regulation in satellite cell activation. *Skelet. muscle* 2, 21. [PubMed: 23046558]
- Golzio C, Martinovic-Bouriel J, Thomas S, Mougou-Zrelli S, Grattagliano-Bessieres B, Bonniere M, Delahaye S, Munnich A, Encha-Razavi F, Lyonnet S, Vekemans M, Attie-Bitach T, Etchevers HC, 2007 Matthew-Wood syndrome is caused by truncating mutations in the retinol-binding protein receptor gene STRA6. *Am J Hum Genet* 80, 1179–1187. [PubMed: 17503335]
- Huggins GS, Bacani CJ, Boltax J, Aikawa R, Leiden JM, 2001 Friend of GATA 2 physically interacts with chicken ovalbumin upstream promoter-TF2 (COUP-TF2) and COUP-TF3 and represses COUP-TF2-dependent activation of the atrial natriuretic factor promoter. *J Biol Chem* 276, 28029–28036. [PubMed: 11382775]
- Jay PY, Bielinska M, Erlich JM, Mannisto S, Pu WT, Heikinheimo M, Wilson DB, 2007 Impaired mesenchymal cell function in *Gata4* mutant mice leads to diaphragmatic hernias and primary lung defects. *Dev Biol* 301, 602–614. [PubMed: 17069789]
- Kammoun M, Souche E, Brady P, Ding J, Cosemans N, Gratacos E, Devriendt K, Eixarch E, Deprest J, Vermeesch JR, 2018 Genetic profile of isolated congenital diaphragmatic hernia revealed by targeted next-generation sequencing. *Prenat Diagn* 38, 654–663. [PubMed: 29966037]

- Kardon G, Ackerman KG, McCulley DJ, Shen Y, Wynn J, Shang L, Bogenschutz E, Sun X, Chung WK, 2017 Congenital diaphragmatic hernias: from genes to mechanisms to therapies. *Dis. Model. Mech* 10, 955–970. [PubMed: 28768736]
- Kling DE, Cavicchio AJ, Sollinger CA, Schnitzer JJ, Kinane TB, Newburg DS, 2010 Nitrofen induces apoptosis independently of retinaldehyde dehydrogenase (RALDH) inhibition. *Birth Defects Res. B Dev. Reprod. Toxicol* 89, 223–232. [PubMed: 20549697]
- Logan M, Martin J, Nagy A, Lobe C, Olson E, Tabin C, 2002 Expression of Cre Recombinase in the developing mouse limb bud driven by a Prxl enhancer. *Genesis* 33, 77–80. [PubMed: 12112875]
- Longoni M, High FA, Russell MK, Kashani A, Tracy AA, Coletti CM, Hila R, Shamia A, Wells J, Ackerman KG, Wilson JM, Bult CJ, Lee C, Lage K, Pober BR, Donahoe PK, 2014 Molecular pathogenesis of congenital diaphragmatic hernia revealed by exome sequencing, developmental data, and bioinformatics. *Proc. Natl. Acad. Sci. USA* 111, 12450–12455. [PubMed: 25107291]
- Longoni M, Lage K, Russell MK, Loscertales M, Abdul-Rahman OA, Baynam G, Bleyl SB, Brady PD, Breckpot J, Chen CP, Devriendt K, Gillessen-Kaesbach G, Grix AW, Rope AF, Shimokawa O, Strauss B, Wieczorek D, Zackai EH, Coletti CM, Maalouf FI, Noonan KM, Park JH, Tracy AA, Lee C, Donahoe PK, Pober BR, 2012 Congenital diaphragmatic hernia interval on chromosome 8p23.1 characterized by genetics and protein interaction networks. *Am J Med Genet A* 158A, 3148–3158. [PubMed: 23165946]
- Major D, Cadenas M, Fournier L, Leclerc S, Lefebvre M, Cloutier R, 1998 Retinol status of newborn infants with congenital diaphragmatic hernia. *Pediatr. Surg. Int* 13, 547–549. [PubMed: 9799371]
- Mendelsohn C, Lohnes D, Decimo D, Lufkin T, LeMeur M, Chambon P, Mark M, 1994 Function of the retinoic acid receptors (RARs) during development (II). Multiple abnormalities at various stages of organogenesis in RAR double mutants. *Development* 120, 2749–2771. [PubMed: 7607068]
- Merrell AJ, Ellis BJ, Fox ZD, Lawson JA, Weiss JA, Kardon G, 2015 Muscle connective tissue controls development of the diaphragm and is a source of congenital diaphragmatic hernias. *Nat. Genet* 47, 496–504. [PubMed: 25807280]
- Merrell AJ, Kardon G, 2013 Development of the diaphragm -- a skeletal muscle essential for mammalian respiration. *FEBS J* 280, 4026–4035. [PubMed: 23586979]
- Mey J, Babiuk RP, Clugston R, Zhang W, Greer JJ, 2003 Retinal dehydrogenase-2 is inhibited by compounds that induce congenital diaphragmatic hernias in rodents. *Am. J. Pathol* 162, 673–679. [PubMed: 12547725]
- Muzumdar M, Tasic B, Miyamichi K, Li L, Luo L, 2007 A global double-fluorescent Cre reporter mouse. *Genesis* 45, 593–605. [PubMed: 17868096]
- Nakao Y, Ueki R, 1987 Congenital diaphragmatic hernia induced by nitrofen in mice and rats: characteristics as animal model and pathogenetic relationship between diaphragmatic hernia and lung hypoplasia. *Cong. Anom* 27, 397–417.
- Noble BR, Babiuk RP, Clugston RD, Underhill TM, Sun H, Kawaguchi R, Walfish PG, Blomhoff R, Gundersen TE, Greer JJ, 2007 Mechanisms of action of the congenital diaphragmatic hernia-inducing teratogen nitrofen. *Am. J. Physiol. Lung Cell. Mol. Physiol* 293, L1079–1087. [PubMed: 17704186]
- Paris ND, Coles GL, Ackerman KG, 2015 *Wtl* and β -*catenin* cooperatively regulate diaphragm development in the mouse. *Dev. Biol* 407, 40–56. [PubMed: 26278035]
- Pasutto F, Sticht H, Hammersen G, Gillessen-Kaesbach G, Fitzpatrick DR, Nurnberg G, Brasch F, Schirmer-Zimmermann H, Tolmie JL, Chitayat D, Houge G, Fernandez-Martinez L, Keating S, Mortier G, Hennekam RC, von der Wense A, Slavotinek A, Meinecke P, Bitoun P, Becker C, Nurnberg P, Reis A, Rauch A, 2007 Mutations in STRA6 cause a broad spectrum of malformations including anophthalmia, congenital heart defects, diaphragmatic hernia, alveolar capillary dysplasia, lung hypoplasia, and mental retardation. *Am J Hum Genet* 80, 550–560. [PubMed: 17273977]
- Perry SF, Similowski T, Klein W, Codd JR, 2010 The evolutionary origin of the mammalian diaphragm. *Respir. Physiol. Neurobiol* 171, 1–16. [PubMed: 20080210]

- Pober BR, 2007 Overview of epidemiology, genetics, birth defects, and chromosome abnormalities associated with CDH. *Am. J. Med. Genet. C Semin. Med. Genet* 145C, 158–171. [PubMed: 17436298]
- Rhinn M, Dollé P, 2012 Retinoic acid signalling during development. *Development* 139, 843–858. [PubMed: 22318625]
- See AW-M, Kaiser ME, White JC, Clagett-Dame M, 2008 A nutritional model of late embryonic vitamin A deficiency produces defects in organogenesis at a high penetrance and reveals new roles for the vitamin in skeletal development. *Dev. Biol* 316, 171–190. [PubMed: 18321479]
- Sefton EM, Gallardo M, Kardon G, 2018 Developmental origin and morphogenesis of the diaphragm, an essential mammalian muscle. *Dev. Biol* 440, 64–73. [PubMed: 29679560]
- Shannon SR, Moise AR, Trainor PA, 2017 New insights and changing paradigms in the regulation of vitamin A metabolism in development. *Wiley Interdiscip. Rev. Dev. Biol* 6.
- Stege G, Fenton A, Jaffray B, 2003 Nihilism in the 1990s: the true mortality of congenital diaphragmatic hernia. *Pediatrics* 112, 532–535. [PubMed: 12949279]
- Todaro GJ, Green H, 1963 Quantitative studies of the growth of mouse embryo cells in culture and their development into established lines. *J Cell Biol* 17, 299–313. [PubMed: 13985244]
- Uezumi A, Fukada S.-i., Yamamoto N, Takeda S.a.i., Tsuchida K, 2010 Mesenchymal progenitors distinct from satellite cells contribute to ectopic fat cell formation in skeletal muscle. *Nat Cell Biol* 12, 143–152. [PubMed: 20081842]
- Valasek P, Theis S, DeLaurier A, Hinits Y, Luke GN, Otto AM, Minchin J, He L, Christ B, Brooks G, Sang H, Evans DJ, Logan M, Huang R, Patel K, 2011 Cellular and molecular investigations into the development of the pectoral girdle. *Developmental Biology* 357, 108–116. [PubMed: 21741963]
- Wat MJ, Beck TF, Hernandez-Garcia A, Yu Z, Veenma D, Garcia M, Holder AM, Wat JJ, Chen Y, Mohila CA, Lally KP, Dickinson M, Tibboel D, de Klein A, Lee B, Scott DA, 2012 Mouse model reveals the role of SOX7 in the development of congenital diaphragmatic hernia associated with recurrent deletions of 8p23.1. *Hum Mol Genet* 21, 4115–4125. [PubMed: 22723016]
- Wilson JG, Roth CB, Warkany J, 1953 An analysis of the syndrome of malformations induced by maternal vitamin A deficiency. Effects of restoration of vitamin A at various times during gestation. *Am. J. Anat* 92, 189–217. [PubMed: 13030424]
- You LR, Takamoto N, Yu CT, Tanaka T, Kodama T, Demayo FJ, Tsai SY, Tsai MJ, 2005 Mouse lacking COUP-TFII as an animal model of Bochdalek-type congenital diaphragmatic hernia. *Proc Natl Acad Sci U S A* 102, 16351–16356. [PubMed: 16251273]
- Yu L, Bennett JT, Wynn J, Carvill GL, Cheung YH, Shen Y, Mychaliska GB, Azarow KS, Crombleholme TM, Chung DH, Potoka D, Warner BW, Bucher B, Lim FY, Pietsch J, Stolar C, Aspelund G, Arkovitz MS, Mefford H, Chung WK, Mendelian UWC, 2014 Whole exome sequencing identifies de novo mutations in GATA6 associated with congenital diaphragmatic hernia. *J. Med. Genet* 51, 197–202. [PubMed: 24385578]
- Yu L, Wynn J, Cheung YH, Shen Y, Mychaliska GB, Crombleholme TM, Azarow KS, Lim FY, Chung DH, Potoka D, Warner BW, Bucher B, Stolar C, Aspelund G, Arkovitz MS, Chung WK, 2012 Variants in *GATA4* are a rare cause of familial and sporadic congenital diaphragmatic hernia. *Human Genetics* 132.
- Yu L, Wynn J, Cheung YH, Shen Y, Mychaliska GB, Crombleholme TM, Azarow KS, Lim FY, Chung DH, Potoka D, Warner BW, Bucher B, Stolar C, Aspelund G, Arkovitz MS, Chung WK, 2013 Variants in *GATA4* are a rare cause of familial and sporadic congenital diaphragmatic hernia. *Hum Genet* 132, 285–292. [PubMed: 23138528]

HIGHLIGHTS

- Pleuroperitoneal fold (PPF) fibroblasts are critical for diaphragm development
- Mutations in PPFs give rise to birth defect Congenital Diaphragmatic Hernias (CDH)
- Mouse PPF fibroblasts can be cultured for multiple passages
- Genetic mutations or drug inhibitors affect PPF growth in vitro similar to in vivo

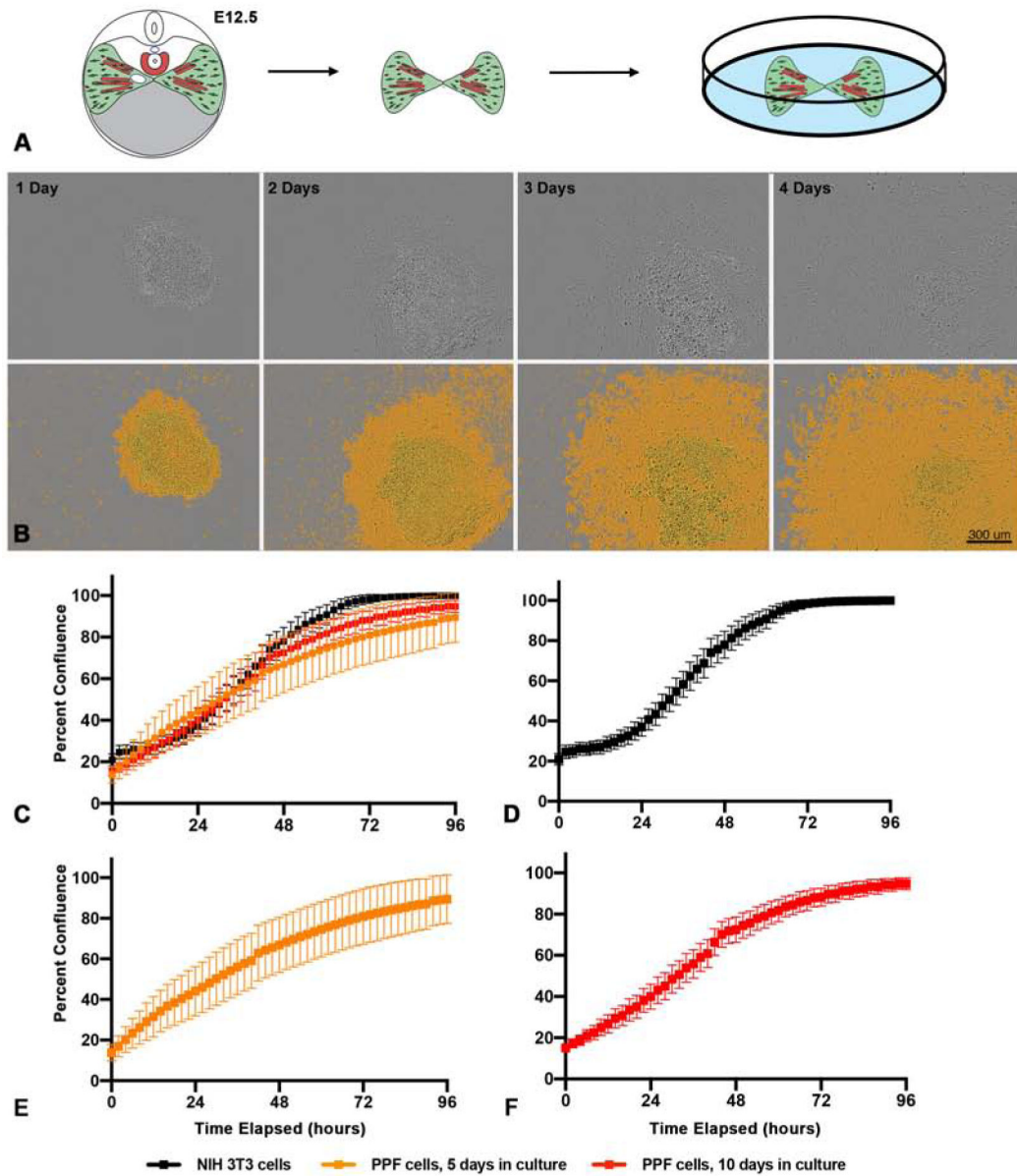


Figure 1. PPFs can be isolated and cultured *in vitro*.

A. E12.5 pairs of PPFs, including muscle progenitors, are dissected from embryos and cultured individually in single wells of 96-well culture plates. **B.** Growth of E11.5 PPFs 1 - 4 d after isolated. Top row, phase-contrast images taken by IncuCyte cell imager. Bottom row, images with IncuCyte-created confluency mask layer to highlight cells (in orange). Scale bar is 300 μ m.

C-F. Comparison of growth of PPFs and NIH3T3 fibroblast (**C**). Growth of NIH 3T3 cells (**D**, $n = 10$ biological replicates), PPF cells after 5 d in culture and 1 passage (**E**, $n = 21$ biological replicates) and PPF cells after 10 d in culture and 2 passages (**F**, $n = 30$ biological replicates). Growth is measured by percent confluency calculated by IncuCyte software and for each timepoint the average of the biological replicates are shown with error bars representing standard error of the mean (SEM).

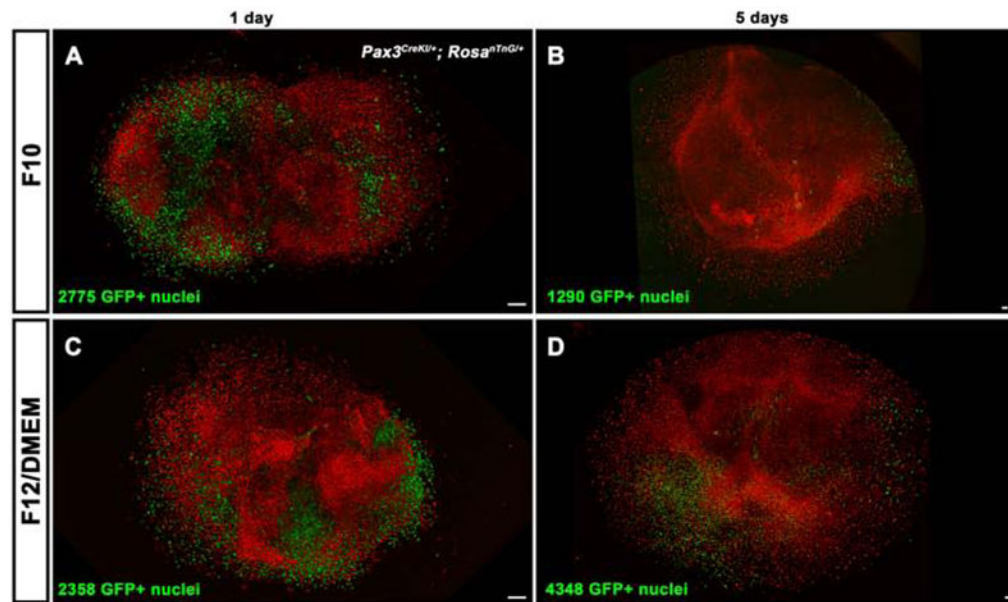


Figure 2. Muscle progenitors and fibroblasts cultured in myogenic media.

Pax3^{CreKl/+}; Rosa^{nTnG/+} E12.5 PPFs, cultured for 1 d (**A**, **C**) or 5 d (**B**, **D**) in F10 with FBS and FGF (**A**, **B**) or F12/DMEM with FBS and FGF (**C**, **D**). F10 media is only suitable to expand PPF fibroblasts, as indicated by the predominance of Tomato+ PPF fibroblasts and reduced numbers of GFP+ myogenic cells by 5 d in culture ($n = 3$) (**B**). F12/DMEM allows expansion of both GFP+ muscle progenitors and Tomato+ PPF fibroblasts as numbers of GFP+ cells increased in 3 of 4 PPF cultures in this media (**D**). Scale bars are 100 μm .

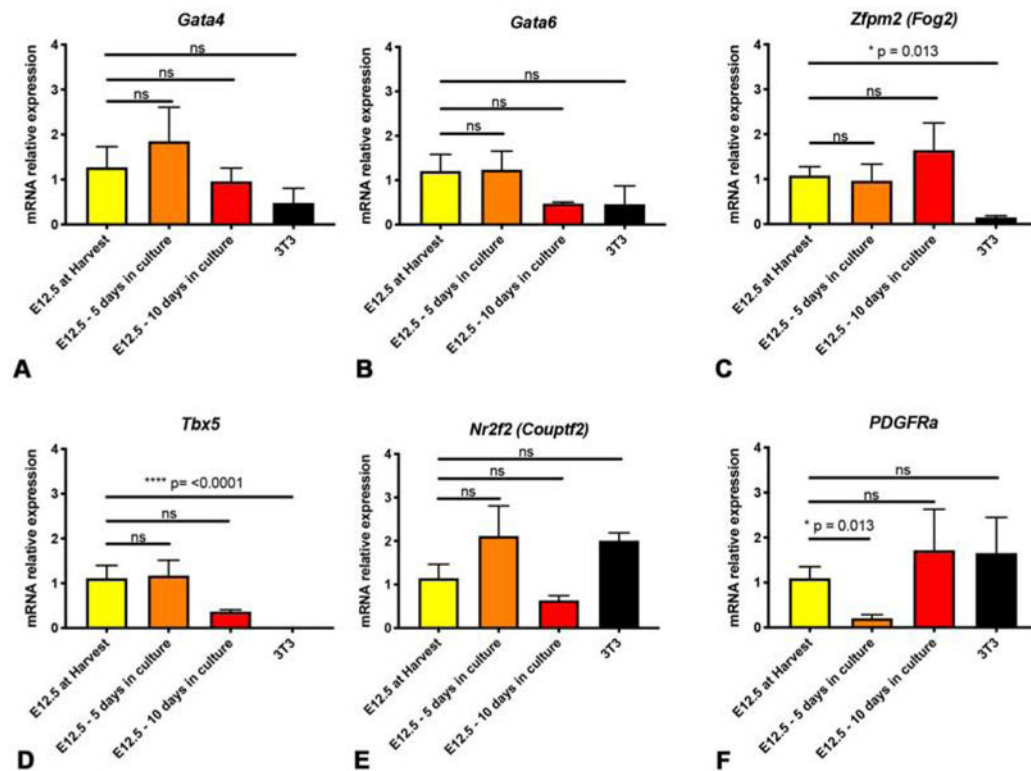


Figure 3. Expression of important diaphragm genes is maintained in E12.5 PPFs during culture. Expression of *Gata4* (A), *Gata6* (B), *Zfpm* (C), *Tbx5* (D), and *Nr2f2* (E) does not statistically differ in E12.5 PPFs when cultured 5 or 10 d. *PDGFRa* is reduced after 5 d in culture, but is not significantly reduced after 10 d in culture (F). NIH 3T3 fibroblasts have lower expression of *Zfpm2* (C) and undetectable levels of *Tbx5* (D). For each experiment, 3 pairs of E12.5 PPFs were pooled or 3 wells of 3T3s were pooled and then 2-5 pools were used for qPCR. Gene expression determined by qRT-PCR, normalized against *18S* gene expression, and then normalized to “at harvest” value, which was set to 1. Significance tested with one-way ANOVA. Holm–Sidak post hoc tests are indicated by * p<0.05, **** p<0.0001. Error bars represent standard error of the mean (SEM).

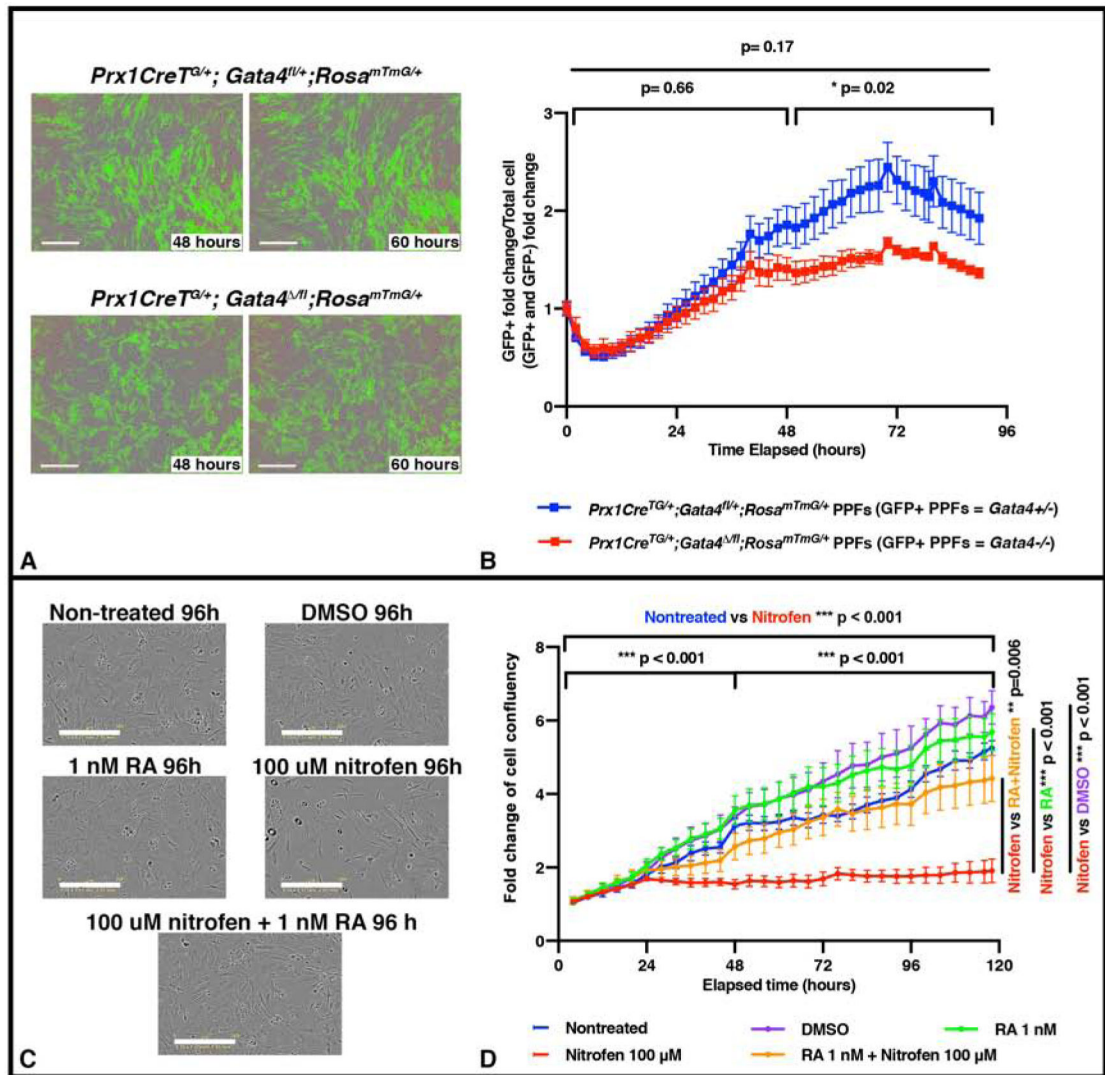


Figure 4. *In vitro* proliferation of PPF fibroblasts is inhibited by genetic mutation and pharmacological inhibitor previously demonstrated to cause CDH *in vivo*.

A-B. E12.5 PPFs isolated from either *Prx1Cre^{Tg+/+}; Gata4^{fl/+}; Rosa^{mTmG/+}* (with GFP+ *Gata4*^{+/-} PPFs, n = 2 biological replicates, 2 technical replicates) or *Prx1Cre^{Tg+/+}; Gata4^{del/fl}; Rosa^{mTmG/+}* (with GFP+ *Gata4*^{-/-} PPFs, n = 3 biological replicates, 2 technical replicates) embryos and cultured after 5 d (one passage) on the IncuCyte ZOOM, with GFP (to measure confluence of GFP+ cells) and phase (to measure confluence of all cells). Representative GFP and phase images shown in (A). The average ratio GFP+ PPF fold change (% confluence at time T/% confluence at time 0) over total PPF + fold change \pm SEM is plotted (B). **C-D.** E12.5 PPFs were cultured after 5 d (and one passage) either untreated (n = 5), treated with DMSO (n = 5), treated with RA, treated with nitrofen (n = 5), or treated with RA plus nitrofen (n = 5) on the IncuCyte ZOOM to track cell confluency via phase images. Representative phase images shown in (C). Average fold change (% confluence at time T/% confluence at time 0) \pm SEM is plotted in (D). Statistical changes in total confluency over time were determined using repeated measure

ANOVA on the log₂ transformed fold change over time, with bars on top of graphs denoting whether comparison was between T=0 to T= total time elapsed, or through the first or last halves of the experiments (**B**, **D**) Bars on side of graph (**D**) are comparing across entire lapsed time. *** P= <0.001, * P= <0.05.

Author Manuscript

Author Manuscript

Author Manuscript

Author Manuscript